Physiol Genomics 30: 44–52, 2007.
First published February 27, 2007; doi:10.1152/physiolgenomics.00070.2006.

Reparative myocardial mechanisms in adult C57BL/6 and MRL mice following injury

R. Haris Naseem,[1] Annette P. Meeson,[1] J. Michael DiMaio,[2] Michael D. White,[2] Justin Kallhoff,[1] Caroline Humphries,[1] Sean C. Goetsch,[1] Leon J. De Windt,[3] Maurice A. Williams,[1] Mary G. Garry,[1] and Daniel J. Garry[1,4,5]

Departments of [1]Internal Medicine and [2]Cardiothoracic Surgery, University of Texas Southwestern Medical Center, Dallas, Texas; [3]Hubrecht Laboratory and Interuniversity Cardiology Institute Netherlands, Royal Netherlands Academy of Arts and Sciences, Utrecht, The Netherlands; [4]Department of Molecular Biology, University of Texas Southwestern Medical Center, and [5]Donald W. Reynolds Cardiovascular Clinical Research Center at UT Southwestern Medical Center, Dallas, Texas

Submitted 24 April 2006; accepted in final form 23 February 2007

Naseem RH, Meeson AP, DiMaio JM, White MD, Kallhoff J, Humphries C, Goetsch SC, De Windt LJ, Williams MA, Garry MG, Garry DJ. Reparative myocardial mechanisms in adult C57BL/6 and MRL mice following injury. *Physiol Genomics* 30: 44–52, 2007. First published February 27, 2007; doi:10.1152/physiolgenomics.00070.2006.—Previous studies have suggested that the heart may be capable of limited repair and regeneration in response to a focal injury, while other studies indicate that the mammalian heart has no regenerative capacity. To further explore this issue, we performed a series of superficial and transmural myocardial injuries in C57BL/6 and MRL/MpJ adult mice. At defined time intervals following the respective injury (*days 3, 14, 30* and *60*), we examined cardiac function using echocardiography, morphology, fluorescence-activated cell sorting for 5-bromo-2-deoxyuridine-positive cells and molecular signature using microarray analysis. We observed restoration of myocardial function in the superficial MRL cryoinjured heart and significantly less collagen deposition compared with the injured hearts of C57BL/6 mice. Following a severe transmural myocardial injury, the MRL mouse has increased survival and decreased ventricular remodeling compared with the C57BL/6 mouse but without evidence of complete regeneration. The cytoprotective program observed in the severely injured MRL heart is in part due to increased cellular proliferation, increased vasculogenesis, and decreased apoptosis that limits the extension of the injury. We conclude that MRL injured hearts have evidence of myocardial regeneration, in response to superficial injury, but the stabilized left ventricular function and improved survival observed in the MRL mouse following severe injury is not associated with complete myocardial regeneration.

myocardial regeneration; cytoprotection; progenitor cells; echocardiography; TUNEL assay; transcriptome analysis

AMPHIBIANS AND TELEOST FISH have a remarkable myocardial regenerative capacity following injury (5, 6, 33). Following the amputation of the ventricular apex in zebrafish, a well-orchestrated molecular and cellular response results in complete myocardial regeneration and an absence of scar formation (33). Studies undertaken in these metazoan models suggest a dynamic balance exists between the fibroproliferative response that produces scar and the regenerative response that produces functional, contractile tissue (6, 33).

Adult mammalian tissues typically have a progenitor or stem cell population that function in the maintenance and regeneration of the tissue in which they reside (8, 11, 38). Bone marrow, skin, liver, skeletal muscle and brain are several examples of adult tissues that harbor somatic progenitor/stem cell populations and are capable of regeneration (8, 11, 38). Recent studies suggest that the adult murine heart also contains such a progenitor cell population and potentially is capable of limited regeneration (3, 10, 22, 28). Analysis of these cardiac progenitor cell populations and the fibroproliferative response following a myocardial injury remains an area of intense interest and investigation (10).

The MRL/MpJ (MRL) mouse strain has been proposed as a model that has an enhanced regenerative capacity. The MRL mouse strain was initially observed to be capable of ear hole closure (following a 2-mm ear hole punch) with minimal scar formation (7, 24). The ear hole closure was considered to be a regenerative response and not wound repair because there was the replacement of multiple tissues (i.e., skin, hair follicles, skeletal muscle, sebaceous glands, cartilage, and vasculature) in the absence of scar formation (7, 24). This reparative process has been associated with the formation of a blastema-like structure (a mass of mesenchymal cells from which new tissue is differentiated) and increased vascularization (7). Recent studies suggest that other tissues in the adult MRL mouse may be capable of regeneration including the heart, brain and spinal cord (21). In contrast, other studies demonstrate that there is no evidence of myocardial regeneration or limited scar formation following reperfusion injury (1) or coronary ligation (29) in the MRL mouse heart.

In the present study, we undertook a series of superficial and transmural myocardial injuries to evaluate the regenerative response in the C57BL/6 (B6) and MRL adult heart. Utilizing an array of technologies, we observed that the adult MRL heart has an enhanced regenerative capacity in response to mild forms of injury (superficial cryoinjury). In response to a severe transmural myocardial injury, the MRL mouse displayed increased survival, decreased remodeling and stabilization of left ventricular performance. However, complete myocardial regeneration was not observed.

MATERIALS AND METHODS

Animals and ear punches. Adult male B6 and MRL mice (Jackson Laboratory) 2–4 mo of age were used in these studies. Mice were bred and housed in cages and all animal protocols were in accordance with our institutional animal care guidelines. A 2-mm ear punch was made

Article published online before print. See web site for date of publication (http://physiolgenomics.physiology.org).

Address for reprint requests and other correspondence: D. J. Garry, NB11.118A, 5323 Harry Hines Blvd., Univ. of Texas Southwestern Medical Ctr., Dallas, TX 75390-8573 (e-mail: Daniel.garry@utsouthwestern.edu).

through the middle of the ears with a metal ear punch. The holes were measured and imaged immediately after they were punched and at weekly intervals using a digital caliper. 5-Bromo-2-deoxyuridine (BrdU, 1 mg/ml) was provided in the drinking water for defined periods following ear hole punch to label proliferating cells.

Myocardial injuries. Three different myocardial injury models were utilized in these studies by three different surgeons in three different laboratories (25, 35, 37). All studies were undertaken in a blinded fashion. A superficial cryoinjury was induced as a nontransmural injury model and either a transmural cryoinjury or a proximal left anterior descending (LAD) coronary artery ligation were used to produce more severe forms of myocardial injury. In all cases, mice were anesthetized with 2% isoflurane, intubated, and ventilated with a small animal ventilator (Harvard Apparatus). A left thoracotomy was performed, and the heart was exposed to induce cryoinjuries consistently in the same area of the left ventricle (LV). A superficial or transmural cryoinjury was induced by exteriorizing the heart and applying a liquid nitrogen cooled probe to the LV for 5 or 15 s, respectively. The size of the probe used to induce injury was 2.18 mm $\times$ 2.52 mm. The resulting injury was easily visualized and measured to be 4.27 $\pm$ 0.5 mm $\times$ 3.88 $\pm$ 0.30 mm. The longer freezing period (15 sec) resulted in deeper transmural injuries.

Alternatively, the proximal LAD coronary artery (immediately after the bifurcation of the left main coronary artery) was ligated with an 8-0 prolene suture (37). Successful occlusion of the LAD was confirmed under a dissecting microscope (Olympus SZ30, Japan) by discoloration of the ischemic area as previously described (37). All animals were monitored closely during the 24-h postoperative period.

Myocardial functional assessment by echocardiography and invasive hemodynamics. Noninvasive transthoracic echocardiograms (General Electric Vivid7 Pro machine equipped with a 12-mHz transducer) were performed in unsedated mice at baseline and 3, 14, 30, and 60 days following injury (35). Motion mode (M-mode) and two-dimensional echocardiographic images were obtained in the parasternal short-axis view. Fractional shortening was calculated from M-mode images as the left ventricular end-diastolic dimension (LVEDD) minus the left ventricular end-systolic dimension (LVESD) divided by LVEDD. Invasive hemodynamic measurements were obtained in isoflurane-anesthetized mice as previously described (39). Following thoracotomy and pericardotomy a 1.4-Fr micromanometer catheter (Millar Instruments) was inserted into the LV. Left ventricular pressure-volume relationships were measured by transiently compressing the inferior vena cava. Parallel volume of each mouse was calibrated by the injection of 10 μl of hypertonic saline into the external jugular vein. The volume calibration of the conductance system was performed as described by Yang et al. (39). Functional analyses were undertaken by two different investigators who were blinded to treatment. We measured LV dysfunction both invasively and noninvasively to quantify the extent of myocardial infarct, using physiologically relevant measurements, in each of these three injury models.

Histology and immunohistochemistry. Adult mice were anesthetized with Avertin and perfused (transcardiac) with 10 ml of 4% paraformaldehyde-PBS as previously described (12, 22). The hearts were harvested and postfixed for 90 min at room temperature, rinsed in diethyl pyrocarbonate-PBS, and paraffin processed. Using rotary microtomy, we cut 5-μm-thick sections and mounted them on Vectabond-treated slides (Vector Labs, Burlingame, CA). Selected sections were stained with either hematoxylin-eosin stain or Masson's trichrome stain. Immunohistochemical detection of selected proteins was undertaken as previously described (12, 15, 17, 22). In brief, sections were dewaxed, hydrated in PBS, blocked with 5% normal goat serum (30 min at room temperature), and incubated with primary antisera diluted in 1% normal goat serum overnight at 4°C in a humid chamber. The following day the sections were washed with PBS, incubated with the respective fluorophore-conjugated secondary antisera (30 min at room temperature), washed with PBS, and coverslipped with Vectashield. Primary antisera used in these studies include rabbit anti-von Willebrand serum (1:150, Novacastra), rabbit antitroponin I (1:500, Chemicon), and a monoclonal anti-BrdU serum (1:25, Roche). The secondary antisera included an FITC-conjugated goat anti-rabbit serum (1:50, Jackson ImmunoResearch), rhodamine goat anti-rabbit serum (1:50, Jackson ImmunoResearch), and FITC-conjugated goat anti-mouse serum (1:50, Jackson ImmunoResearch). The nuclei were stained with propidium iodide (50 ng/ml, Molecular Probes) (17). The TdT-mediated dUTP nick end labeling (TUNEL) assay was performed with an in situ cell death detection kit (DeadEnd colorimetric TUNEL system, Promega) according to the manufacturer's instructions as previously described (17).

Histological measurement of infarct area and scar formation. Quantification of collagen deposition following injury was performed with histological sections stained with Masson's trichrome. The region of injury was determined by computer-based quantification (Adobe Photoshop) of the scar vs. measurements of the full thickness of the LV. A ratio of collagen deposition-LV wall thickness was calculated to derive the percentage of LV wall with collagen deposition (as a measure of scar) involvement.

BrdU labeling and detection of BrdU-labeled cells by fluorescence-activated cell sorting. BrdU (1 mg/ml) was administered ad libitum in the drinking water of animals that were used as controls and those that were subjected to myocardial injury. At specified times following injury, selected animals were perfused transcardially with ice-cold PBS. Hearts were digested with pronase (10 mg/ml) at 38°C with gentle agitation for 45 min. The tissue slurry was triturated in complete DMEM, and the supernatant (containing the cells) was removed and passed over a Percoll density centrifugation gradient (40%/70%) and resuspended at 10^6 cells/ml Hanks' buffer containing 2% fetal calf serum. Cells were stained with the BrdU antibody using the BD Pharmingen FITC BrdU Flow Kit as outlined in the manufacturer's instructions. BrdU-labeled cells were quantified and isolated by fluorescence-activated cell sorting (FACS; MoFlo, Cytomation); RNA was isolated (Optimum RNA Isolation Kit, Ambion), amplified, and hybridized to the Affymetrix 430 Mouse GeneChip (see *Affymetrix array hybridization and analysis*).

RNA isolation and RT-PCR analysis. Total RNA was isolated from cells collected by FACS or from the LV of uninjured or injured adult mice using TriPure isolation reagent (Roche, Basel, Switzerland) as previously described (9, 15, 22, 23, 25, 28). RNA from FACS-sorted cells was then amplified as previously described (9, 23). Using conditions in which the abundance of each amplified cDNA varied linearly with input RNA, we performed semiquantitative RT-PCR in a final volume of 20 μl (9, 15, 23, 25). All primers spanned an intron, and the sequences are provided in Supplemental Table S1. (The online version of this article contains supplemental material.) For quantitative RT-PCR analysis, oligo d(T)-primed single-strand cDNA was synthesized from 5 μg of total RNA using Superscript II (Invitrogen). Gene-specific primer sets were designed such that the primers spanned an intron and possible genomic contamination could be detected by size difference. Real-time PCR was performed using an ABI 7900HT instrument and SYBR Green PCR Master Mix. The sequences of the primers used are provided in Supplemental Table S1.

Affymetrix array hybridization and analysis. Oligonucleotide array hybridizations were carried out according to the Affymetrix protocol as previously described (9, 15, 23, 25). Briefly, the double-stranded cDNA was converted to biotin-labeled cRNA by using the Enzo BioArray high-yield RNA transcript labeling kit (Enzo Biochem). The purified biotin-labeled cRNA was then fragmented with Affymetrix fragmentation buffer for 35 min at 95°C. Labeled fragmented cRNA (15 μg) was then hybridized to the high-density oligonucleotide Murine Genome Array 430 GeneChip (Affymetrix) (pooled RNA isolated from 3 animals/array). After 16 h of hybridization, the array was washed, stained, and scanned according to the manufacturer's protocol. Array quality assessment and expression values were acquired with DNA-Chip Analyzer (dChip) model-based analysis of

multiple arrays. This method utilizes invariant-set normalization and model-based expression indexes (MBEI) with standard error (SE) to measure accuracy. Comparative analysis was performed by using MBEI and SE to construct a 90% confidence interval of fold change (9, 15).

RESULTS

Ear hole closure in the MRL mouse. In the present study, we confirmed that the adult MRL mice are capable of ear hole closure within a 1-mo period unlike the age- and sex-matched B6 mice that served as controls ($n = 6$ for each group; Supplemental Fig. S1). The ear hole closure in the MRL mouse is a regenerative process as the architecture of a number of lineages (i.e., skin, cartilage, skeletal muscle, peripheral nerve, and vasculature) are labeled with BrdU (representing cellular proliferation) without evidence of scar formation as previously reported (see Supplemental Fig. S1) (7, 24).

MRL mice with superficial myocardial injuries have restored heart function. Regenerative capacity in the MRL mouse heart is dependent upon the severity of the injury. Additional reports suggest that other tissues such as the heart and spinal cord in the MRL mouse were also capable of regeneration (21). In contrast, the notion of cardiac regeneration in the MRL mouse has recently been challenged in ischemic models of injury (1, 29). To evaluate this issue in the adult heart and in this mouse model, we undertook a comprehensive analysis of three different modes of myocardial injury in B6 and MRL age- and sex-matched adult mice. Reproducible superficial cryoinjuries of B6 and MRL hearts were performed without any significant differences in survival ($n = 20$ for each group). At selected time periods following this superficial myocardial injury (*days 3, 14, 30,* and *60*), the LV function was evaluated, and mice were killed for morphological analysis of the injured hearts ($n = 3$ for each group). At all time periods, there was a reduced fibroproliferative (i.e., collagen deposition) response to the superficial myocardial injury in the MRL mouse compared with B6 controls. Representative gross images (Fig. 1, *A* and *B*) and histological analysis with quantification of the ventricular collagen deposition (Fig. 1, *C–E*) further emphasize the limited fibroproliferative response (i.e., scar formation) in the superficially injured MRL heart (6-fold difference) compared with the B6 control 2 mo postinjury (Fig. 1*E*). According to transthoracic echocardiography in unanesthetized mice, this superficial injury resulted in a modest decrease in LV function by *day 3* postinjury (Fig. 1*F*). No improvement of LV function was observed in the B6 mice [fractional shortening (FS) = 45% ± 2% at 2 mo, $n = 6$; Fig. 1*F*)]. In contrast, 2 mo following injury there is restoration of myocardial function in the injured MRL mice (FS = 73 ± 4%, $n = 6$ for each group) (Fig. 1*F* and Table 1). To further emphasize the myocardial recovery of the injured MRL mouse, M-mode echocardiography of the same MRL mouse is shown in Fig. 1*G* at *day 14* postinjury, which

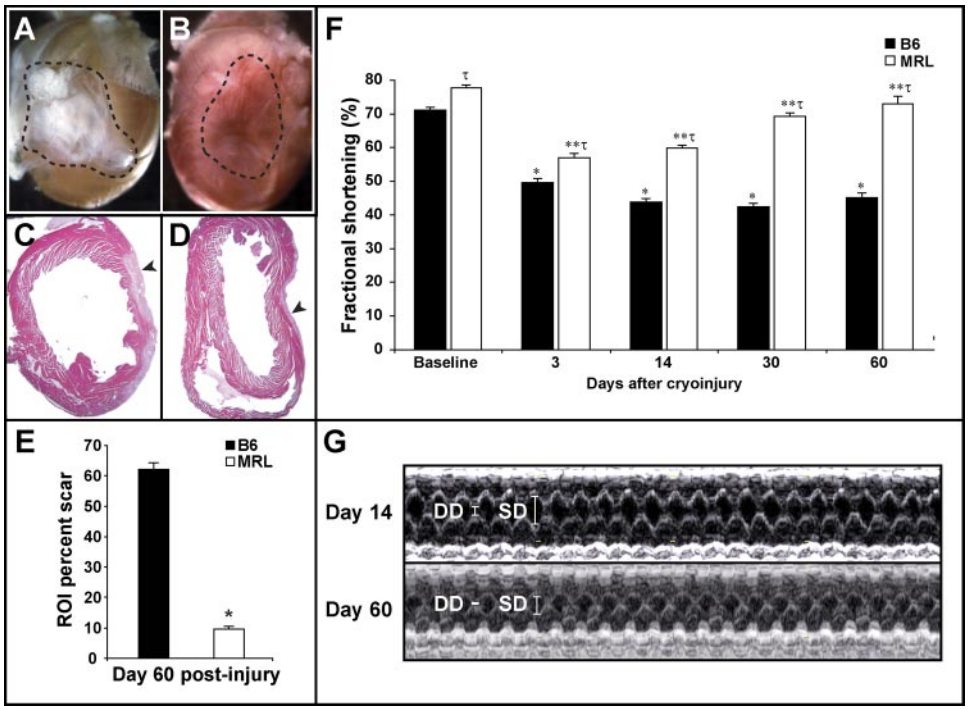

Fig. 1. Limited scar formation and restoration of function in the superficially injured MRL/MpJ (MRL) heart. Two months following a superficial myocardial cryoinjury, a fibrotic scar is evident in the C57BL/6 (B6) mouse (*A*) but only a highly vascular (blastema-like) region is evident in the MRL heart (*B*). Note the black dashed line outlines the region of injury (*A* and *B*). Histologically, the superficial cryoinjury in the B6 mouse heart is evident as it is associated with collagen deposition (arrowhead) (*C*), unlike the minimal fibrosis observed in the MRL heart (*D*) at *day 60* postinjury (arrowhead). Quantification of collagen deposition (representing scar formation) using histological sections [region of interest (ROI) was determined by computer-based quantification of the scar vs. the full thickness of the left ventricle (LV)] reveals a 6-fold decrease in scar formation of the 60-day postinjured MRL heart compared with the B6 control (*E*) ($n = 3$, $^*P < 0.05$). Following a superficial cryoinjury to the heart, the MRL mice have restoration of function within a 60-day period according to echocardiography in unanesthetized mice (*F*). Representative motion (M)-mode echocardiography of the same MRL mouse 14 days and 60 days postinjury. Note increased LVDD and decreased systolic function in the injured MRL heart at *day 14* postinjury with restoration of function by *day 60* (*G*) (DD, LV end-diastolic dimension; SD, LV end-systolic dimension). Data presented as means ± SE. *Significant differences of B6 compared with baseline B6. **Significant differences of MRL compared with baseline MRL. τSignificant differences between MRL and B6 at the same time period postinjury. *, **, τ, $P < 0.05$.

Table 1. *Data summary of the injury models*

Parameter	Mild Cryoinjury		Severe Cryoinjury		Severe Ischemic Injury	
	B6 response	MRL response	B6 response	MRL response	B6 response	MRL response
Survival	++++	++++	++	++++	0	++++
Scarring	++	0	++++	+++	++++	++
Remodeling*	+	0	+++	+	++++	+
LV functional Improvement						
Echocardiography	NC	++++	↓	++		++
Catheter-based analysis	ND	ND	↓	++	ND	ND
Cellular proliferation						
BrdU-labeled cells (FACS)	ND	ND	ND	ND	+	++
BrdU-labeled cardiomyocytes	ND	ND	ND	ND	+	++
TUNEL-positive cells	ND	ND	++	+	ND	ND
Border-zone vascularization	ND	ND	+	++	ND	ND
Regenerative molecular program	ND	ND	ND	ND	+	++

*Remodeling represents chamber dilation and infarct extension. NC, no change; ND, not done; ↓ = decrease; B6, C57BL/6; MRL, MRL/MpJ; LV, left ventricle; BrdU, 5-bromo-2-deoxyuridine; FACS, fluorescence-activated cell sorting; TUNEL, TdT-mediated dUTP nick end labeling.

reveals myocardial dysfunction but restoration of function by *day 60*.

MRL mice with severe myocardial cryoinjuries have decreased remodeling. In the present study, we performed a more severe reproducible transmural cryoinjury in the two strains of mice. The transmural cryoinjury in B6 mice resulted in a progressive dilatation of the LV and a progressive deterioration in myocardial function as measured by echocardiography and catheter-based hemodynamics (Fig. 2, Supplemental Fig. S2 and Table 1). In contrast, the transmural cryoinjured MRL mouse displayed no evidence of LV dilatation and had compensatory septal hypertrophy ($n = 3$ for each group) and stabilization of myocardial function without deterioration during the postinfarct period (FS = 45 ± 6% at *day 3* vs. 49 ± 6%; $n = 6$ for each group; Fig. 2, Supplemental Fig. S2, and Table 1).

Mechanistically, limited LV dilatation, the stabilization of LV function and improved survival are due, in part, to decreased apoptosis of the severely cryoinjured MRL heart (Fig. 2 and Supplemental Fig. S3) and increased vascularization in the border region (Fig. 2 and Supplemental Fig. S4). We observed fewer TUNEL-positive cells in the 3-day (Fig. 2*E*) and 30-day (Fig. 2*F*) injured MRL hearts compared with the B6 hearts at 3 (Fig. 2*C*) and 30 days (Fig. 2*D*) postinjury. Quantification of TUNEL-positive cells revealed that MRL hearts at both 3 and 30 days postinjury had threefold fewer TUNEL-positive cells associated with the injured heart compared with the B6 hearts at the same time points (Fig. 2*G*).

MRL mice with severe transmural ischemic myocardial injuries have increased survival and decreased remodeling. We undertook studies to examine the response of the MRL heart to a severe transmural coronary artery ligation-induced injury. Ligation of the proximal LAD coronary artery in MRL mice resulted in decreased remodeling (i.e., decreased LV dilation), stabilization of myocardial function, and greater survival (Fig. 3 and Supplemental Fig. S5). In contrast, the B6 mice had evidence of increased severity of the coronary ligation-induced injury model, resulting in remodeling, progressive LV dysfunction, and decreased survival with no B6 mice surviving beyond a 1-mo period postinjury ($n = 18$ surviving MRL mice at *day 30* with no spontaneous deaths through 90 days postinjury; Fig. 3 and Table 1). Importantly, complete restoration of function was not observed in the MRL mouse model following the severe transmural injury (i.e., coronary ligation injury) ($n = 7$, Fig. 3 and Supplemental Table S2). Histological analysis revealed the presence of collagen deposition representing an intact or mature scar associated with the injured MRL heart by 2 mo following transmural ischemic injury (i.e., LAD coronary artery ligation injury; $n = 3$ for each group; Fig. 3).

Continuous administration of BrdU to B6 and MRL mice for a 1-mo period following a LAD coronary artery transmural injury was undertaken to evaluate the myocardial regenerative capacity of the adult injured heart. Using immunohistochemical techniques and antisera to detect BrdU-positive nuclei representing cells that had proliferated and troponin I as a cardiomyocyte marker, we evaluated the MRL and B6 heart 30 days following a severe coronary artery ligated injury. We observed approximately a twofold increase (23.7 ± 1.9% in B6 vs. 38.4 ± 5% in MRL hearts, $n = 4$ for each group, $P < 0.05$) in the number of BrdU/troponin I-positive cardiomyocytes in the border region of the 30-day postinjured B6 and MRL hearts (Fig. 4, *A* and *B*, and Supplemental Fig. S6). These results were further supported by FACS to quantify and sort BrdU-positive cells (representing cardiomyocytes and noncardiomyocytes that underwent a proliferative event) from 30-day postinjured MRL and B6 hearts (Fig. 4*C*). We observed a twofold increase ($n = 3$ for each group, $P < 0.05$) in the number of BrdU-positive cells in the injured MRL hearts compared with the injured B6 hearts (Fig. 4*D*). These BrdU-positive cells were FACS sorted from the 30-day injured hearts and analyzed by transcriptome and RT-PCR analyses (Fig. 4, *E* and *F*). Transcripts present in the BrdU-positive cell population isolated from the injured MRL heart were compared with transcripts from adult cardiomyocytes and embryonic cardiomyocytes (embryonic *day 9.5*) that have been analyzed in detail as previously described (23). These analyses were undertaken to determine patterns of transcript expression in the MRL heart that are specific to the adult and embryonic cardiomyocyte populations. BrdU-positive cells from the injured MRL heart express transcripts that further support the proliferation of cardiomyocytes (Casq1, Dag1, Mesp1, Ttn) as well as other lineages [endothelial (Amot and Edf1) and fibroblasts] (Fig. 4*E*). These transcriptome results are further confirmed by RT-PCR analysis of RNA isolated from the BrdU-positive cells (Fig. 4*F*).

Transcriptional signature of the injured/regenerating B6 and MRL hearts. Our studies supported the hypothesis that the MRL heart had an improved reparative capacity compared with the C57BL/6 controls. The MRL mice had improved survival,

stabilized cardiac function, increased cellular proliferation, and decreased remodeling in response to severe transmural myocardial injuries (Table 1). The mechanistic regulation of these responses (i.e., decreased remodeling, increased cellular proliferation, etc.) are complex and incompletely understood. To gain an enhanced understanding of the molecular program that may contribute to the improved reparative capacity of the transmural injured MRL hearts, we undertook a transcriptome

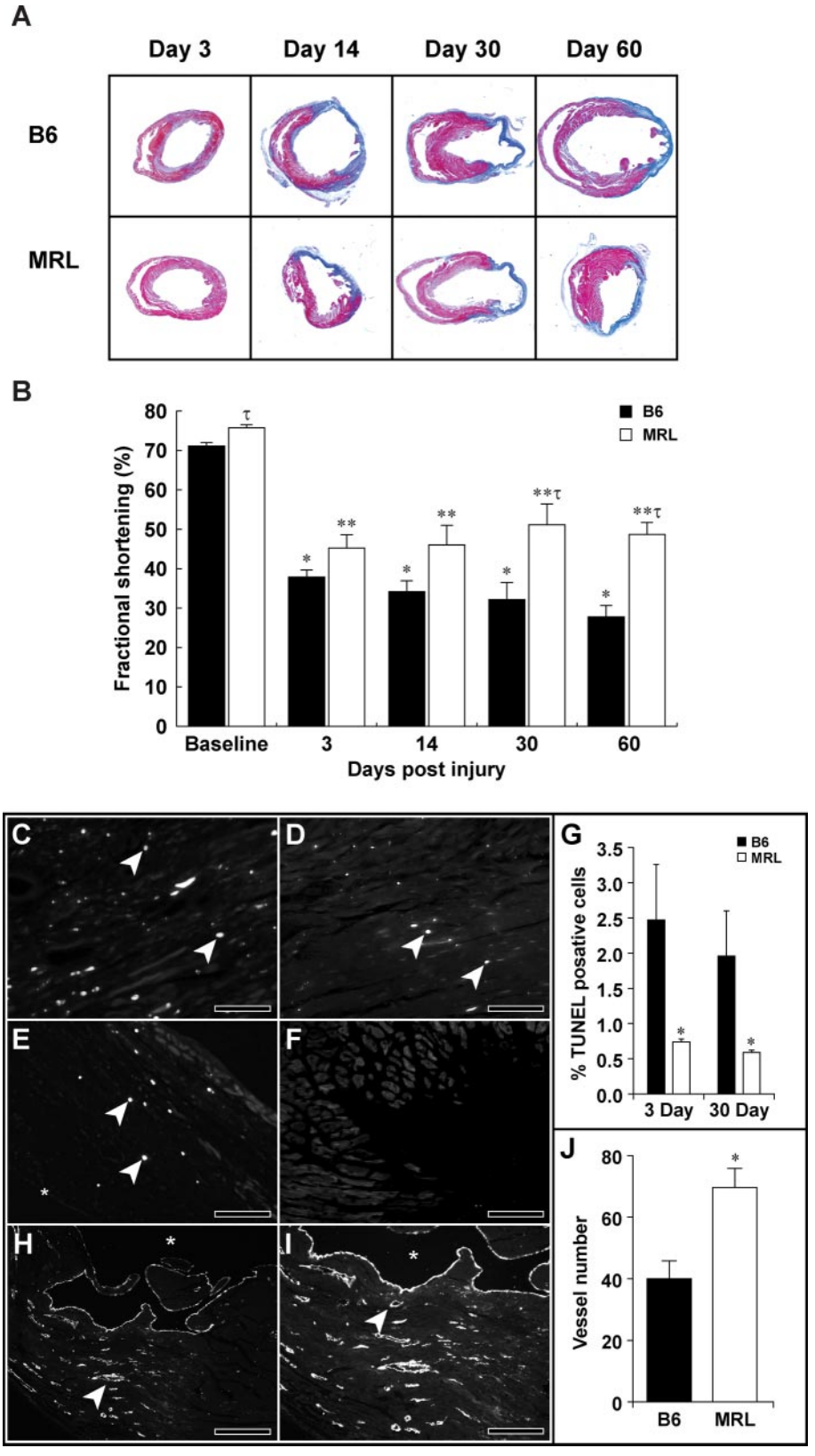

Fig. 2. Stabilized cardiac function and decreased remodeling in the MRL heart following transmural cryoinjury. Age- and sex-matched B6 and MRL mice underwent transmural cryoinjury. At defined time intervals, the injured mice underwent functional assessment by echocardiography and were subsequently killed. Histological analysis revealed progressive extension of the infarct and LV dilation (remodeling) in the B6 injured heart compared with MRL hearts, which showed stabilization of scar after the initial injury, no LV cavity dilation, and the presence of compensatory hypertrophy of the ventricle adjacent to the site of injury (*A*). There was progressive deterioration of the severely injured heart function in the B6 mice, whereas the MRL mice showed modest improvement and then stabilization of function after the transmural myocardial cryoinjury (*B*). Decreased TdT-mediated dUTP nick end labeling (TUNEL)-positive cells were observed in the 3-day (*E*) and 30-day (*F*) postcryoinjured MRL hearts compared with the B6 hearts at 3 days (*C*) and 30 days (*D*) postinjury. TUNEL-positive cells (arrowheads in *C*, *D*, and *E*) are detected by an FITC-conjugated secondary antibody, and results are quantitated in *G* (means ± SE, $*P < 0.05$). Increased vascularization, as measured by von Willebrand immunohistochemical signal (arrowheads in *H* and *I*), was observed in the border region of the MRL 30-day postcryoinjured heart at low magnification (*H*) and high magnification (*I*) compared with the B6 control (see Supplemental Fig. S4); *LV cavity. Data are quantitated in *J* (40.5 ± 4.0 vessels per field in B6 vs. 69.5 ± 6.0 vessels per field in MRL, $*P < 0.05$). Scale bars = 100 μm for *C–H* and 200 μm for *I*.

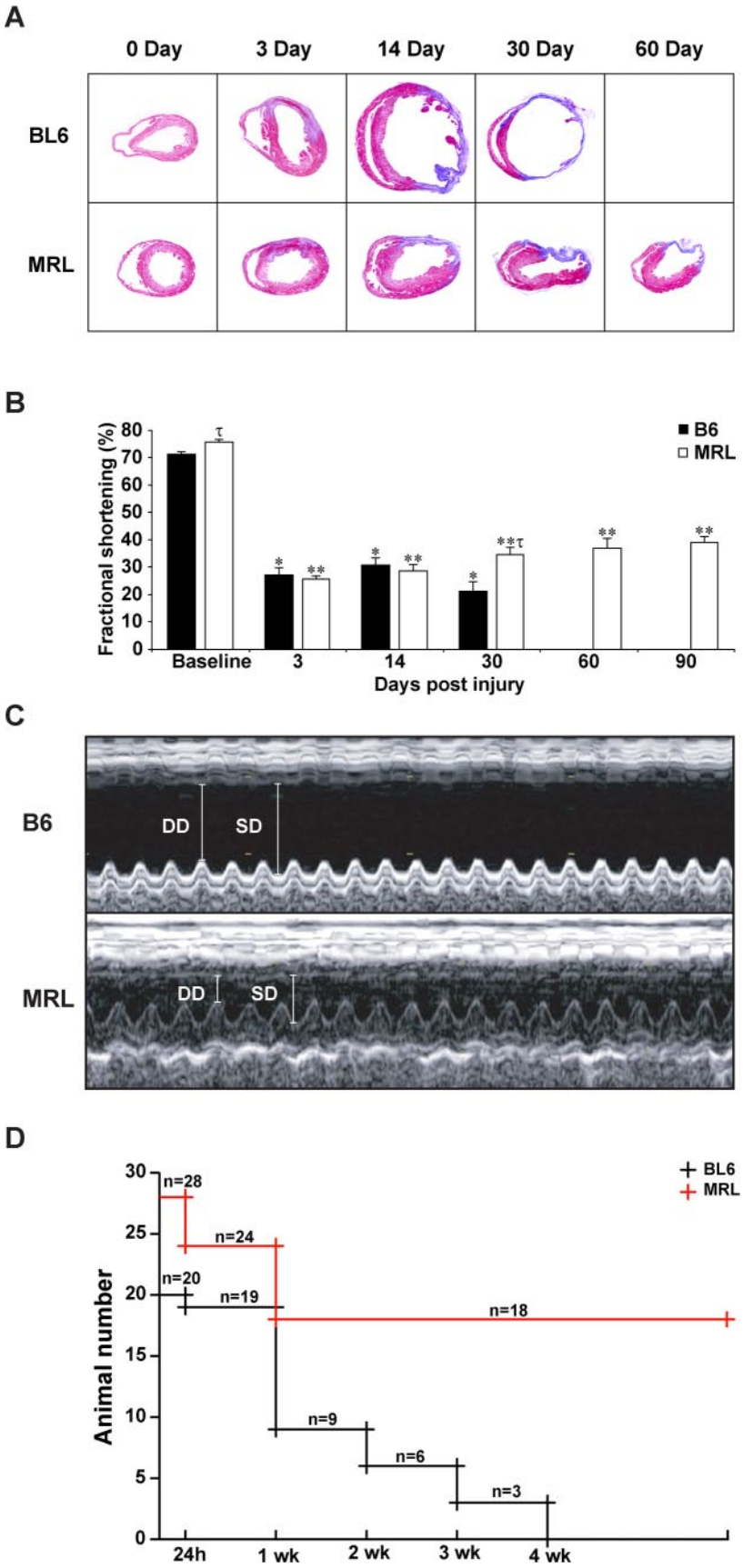

Fig. 3. Improved survival, function, and decreased remodeling in the MRL heart following coronary artery ligation. Age- and sex-matched B6 and MRL mice underwent left anterior descending (LAD) coronary artery ligation. At defined time intervals, the injured mice underwent functional assessment using echocardiography and then were killed. Histological analysis revealed progressive extension of the infarct and LV dilation (remodeling) in the B6 injured heart compared with MRL hearts, which showed stabilization of scar after the initial injury, no LV cavity dilation, and the presence of compensatory hypertrophy of the ventricle adjacent to the site of injury (*A*). Quantitation of the collagen deposition in both strains 30 days following injury is presented in Supplemental Fig. S5. Improved survival of the MRL mice was observed with respect to the B6 controls (no survival of B6 mice beyond the 30 days postinjury period was observed) (*A, B,* and *D*). There was progressive deterioration of the severely injured heart function in the B6 mice, whereas the MRL mice showed modest improvement and then stabilization of function after the LAD coronary artery ligation-induced myocardial injury (*B*). Data presented as means ± SE. *Significant differences of B6 compared with baseline B6. **Significant differences of MRL compared with baseline MRL. τSignificant differences between MRL and B6 at the same time period postinjury. *, **, τ, $P < 0.05$. Representative motion (M)-mode images taken from B6 and MRL mice 1 mo after severe myocardial injury revealed LV cavity dilatation with severely depressed LV function in the B6 mice. MRL hearts showed normal cavity size with significantly improved LV function compared with B6 mice (*C*). Kaplan-Meier survival curve reveals increased survival of MRL mice compared with B6 controls following coronary artery ligation-induced injury. Note that no B6 mice survive beyond the 30-day postinjury period (*D*).

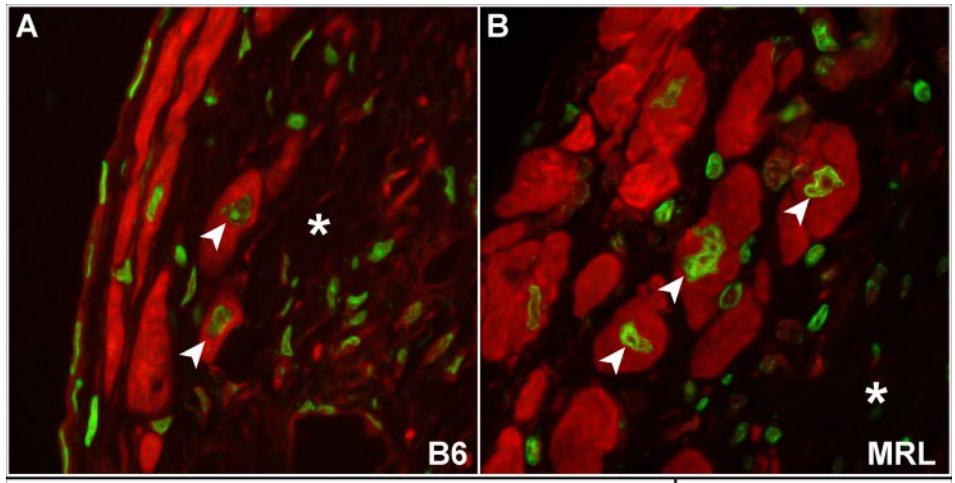

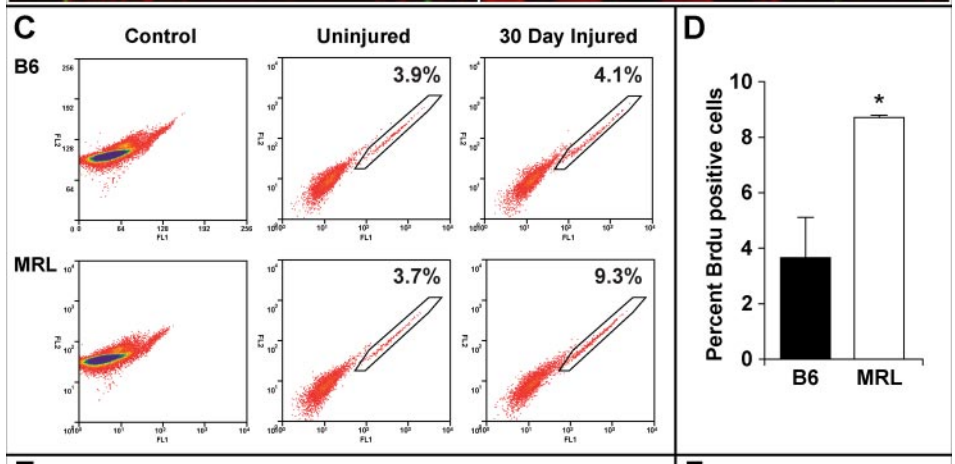

E

Present/Absent calls for MRL, ACM, ECM

Title	Symbol	MRL	ACM	ECM
angiomotin	Amot	P	P	P
bone morphogenic protein 5	Bmp5	P	A	A
calsequestrin 1	Casq1	P	P	P
cytochrome c oxidase, subunite VIIIc	Cox8c	P	P	A
dystroglycan 1	Dag1	P	P	P
endothelial differentiation-related factor 1	Edf1	P	P	P
forkhead box C1	Foxc1	P	A	A
forkhead box P1	Foxp1	P	A	P
mesoderm posterior 1	Mesp1	P	A	A
regulator of G-protein signaling 3	Rgs3	P	A	P
sonic hedgehog	Shh	P	A	A
tropomyosin 3, gamma	Tpm3	P	P	P

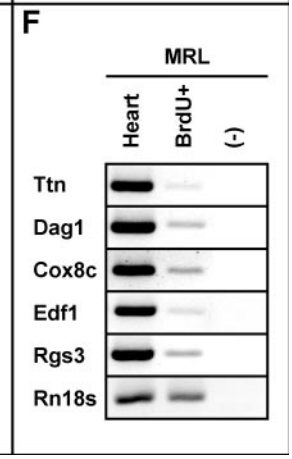

Fig. 4. Regenerative capacity of the adult heart. Adult mice were exposed to continuous (30-day period) 5-bromo-2-deoxyuridine (BrdU) administration (control mice received no BrdU administration and no injury) following no injury (uninjured) or a transmural LAD ligation-induced injury. Representative images of hearts 30 days postinjury that were immunohistochemically costained for BrdU (green) and troponin I (red) reveals evidence of myocardial regeneration with BrdU-labeled cardiomyocytes (arrowheads) (*A* and *B*, *area of injury). Following transmural LAD ligation-induced injury, MRL and B6 mice received continuous BrdU administration for a 30-day period to label proliferating cells. BrdU-pulsed cells from uninjured and 30-day postinjury mice were quantitated and sorted by fluorescence-activated cell sorting (FACS). The percentage of BrdU-positive cells in the gated region is indicated in the *top right* corner of the respective panels (*C*) and quantitated in the *far right* panel (means ± SE, $*P < 0.05$) (*D*). RNA was isolated from FACS-sorted BrdU-positive cells, amplified, and hybridized to the Affymetrix 430 GeneChip. Expression of selected transcripts in the BrdU-positive cells isolated from the injured MRL heart was compared with expression in adult cardiomyocytes (ACM) and embryonic *day 9.5* embryonic cardiomyocytes (ECM) (*E*). Using Affymetrix MAS 5.0 software to analyze the microarray data, we determined selected transcripts to be significantly expressed (designated as P for present) or absent (designated A for absent). Expression data in the BrdU-sorted cells were confirmed by RT-PCR analysis (*F*). Note expression of cardiomyocyte transcripts in the BrdU-positive cells isolated from the respective injured adult hearts using transcriptome and RT-PCR analyses reveals that the BrdU-labeled cells isolated from the injured MRL heart express cardiac transcripts. RNA isolated from the adult MRL heart (heart) is used as a positive control and (−) represents the lack of reverse transcriptase for the RT-PCR negative control (*F*).

analysis using Affymetrix array technology. At defined time periods following an LAD coronary artery ligation-induced myocardial injury, B6 and MRL mice underwent echocardiography, and hearts were harvested and stored for a maximal period of 30 days at −80°C. Total RNA was isolated from individual hearts, labeled, and hybridized to the Affymetrix GeneChip. Using this technology, we observed approximately similar numbers of transcripts dysregulated in the injured B6 and MRL mice *day 3* following injury (1,120 in BL/6 and 1,278 in MRL transcripts having a twofold up- or downregulation compared with their respective uninjured controls). In contrast, *day 30* following injury the B6 injured heart had fivefold more dysregulated transcripts with a majority (95%) of the transcripts downregulated (see Supplemental Table S3). These transcriptome results further support the findings that the MRL mice that have received a transmural myocardial injury have decreased remodeling, stabilization of cardiac function, and improved survival compared with the B6 mice. The 30-day injured MRL heart transcriptome has an upregulation of transcripts broadly associated with cytoprotection (Cygb), vasculogenesis (Edr1), extracellular matrix (Rhbs1, Sdc4, Timp1, Prg4, Fn1, Bgn, Ctss, Tnc), cardiac structural transcripts (Myh7, Myl7, Myl9), transcriptional regulators (Dlx6, Jmjd1), signaling (Sfrp2, Rgs2, Dscr3, Dkk3, Thbs), gap junctions

(Gja1), growth factors/chemokines (Socs3, Ctgf, Ccrl2, Tgfb1, Fstl), cell cycle regulators (Cdkn1a, Son), and factors involved in oxidative stress protection (Sod1, Mt2, Mt1, Gpx3) (Supplemental Tables S4 and S5). QRT-PCR analysis was performed in triplicate from pooled samples to confirm the expression of selected transcripts in the MRL postinjured hearts (Supplemental Fig. S7).

These transcriptome results further establish that molecular programs direct cellular adaptations (i.e., vascularization, cytoprotection, decreased apoptosis, decreased remodeling) that may limit infarct extension (at the border region) in the MRL injured heart. Additionally, the transcriptome results support the notion that a permissive milieu (expression of survival factors such as growth factors/chemokines) results in improved survival of the MRL mouse but does not induce a cascade of gene expression that promotes complete myocardial regeneration.

DISCUSSION

Diverse animal models such as the newt and the zebrafish are capable of limited myocardial regeneration in response to an injury (5, 6, 33). This ability for regeneration of the injured heart is due, in part, to a limited fibroproliferative response resulting in an absence of collagen deposition (5, 6, 33). In the present study, we comprehensively examined the capacity of two strains of mice for myocardial regeneration in response to multiple modes of injury (Table 1). In these studies, the MRL mouse heart was capable of restoration of function and limited collagen deposition following a superficial myocardial injury. The ability for myocardial regeneration, however, is more limited than initially proposed (7, 21, 24). In the present study, we observed that a transmural myocardial injury in MRL mice was associated with improved survival, stabilization of myocardial function, and decreased ventricular remodeling compared with control mice, but the transmurally injured MRL mice were unable to completely regenerate the injured myocardium.

Multiple lines of evidence presented in this study support the conclusion that the adult heart is capable of limited regeneration. First, the superficially injured MRL heart is capable of functional restoration with limited collagen deposition. These results may be comparable to the regenerative response observed in the zebrafish. While the MRL mouse is capable of ear hole closure, the zebrafish is capable of fin regeneration (27, 31, 32). Furthermore, amputation of the apical 20% of the zebrafish ventricle (a mild to moderate injury) results in the formation of a clot at the amputation site, the formation of a blastema (vascularized region of mesenchymal cells), and complete myocardial regeneration within a 2-mo period (33). In the present study we observed a similar response in the superficially injured MRL heart. Furthermore, the zebrafish (or the newt) do not have the capacity for complete regeneration following a more severe myocardial injury (involving 50% or more of the ventricle).

Direct evidence for myocardial regeneration in the adult heart is provided by the presence of BrdU-positive cardiomyocytes and the molecular analysis of FACS-sorted BrdU-positive cells that express cardiomyocyte restricted proteins. Continuous administration of myocardially injured mice with BrdU revealed that a number of cells underwent proliferation in response to the injury but only a subpopulation of cells differentiated to form cardiomyocytes. The source(s) of the cells that repopulated the injured adult heart potentially includes resident or extracardiac progenitor cell populations. Previous studies by our laboratory and others have identified putative progenitor cell populations that are resident in the adult heart based on the expression of Abcg2, cKit, or Sca-1 (3, 22, 28). In addition, previous studies have reported the contribution of extracardiac cells for repair of the injured human and mouse heart, although the extent and the physiological relevance for this contribution are controversial (2, 4, 14, 19, 20, 26, 30, 36).

The conclusion that the MRL mouse has improved survival following a severe transmural myocardial injury is based on the induction of a molecular response that results in increased vascularization, decreased level of apoptosis, lack of LV dilatation (i.e., remodeling), and limited myocardial regeneration (Table 1). In the present study, the transcriptome analysis further supported the induction of a cytoprotective program, increased vasculogenesis, and the exposure of growth factors/chemokines that we hypothesize promotes limited myocardial regeneration in the injured MRL mouse. One factor that was significantly upregulated in the MRL heart early following injury includes tenascin C (15, 16, 34). Tenascin C has been associated with regeneration and functional improvement following injury (18). Tenascin C is markedly upregulated in the blastema of the regenerating limb of the newt, the regenerating ear of the MRL mouse, as well as regenerating skeletal muscle in the mouse (15, 16, 18). Tenascin C has been proposed to limit scar formation by inhibiting the activation of T lymphocytes and the secretion of proinflammatory cytokines such as IL-2 (16, 34). In addition, this protein has been further shown to maintain an undifferentiated state of progenitor cell populations through the modulation of the proadhesive effects of laminin, fibronectin, and collagens (13, 16, 34). Future studies will be necessary to further examine whether administration of tenascin C during the acute period following myocardial injury may limit the fibroproliferative response and promote an increased regenerative response.

Previous studies have emphasized the balance between regeneration and the fibroproliferative response (i.e., scar formation) (10, 33). While the fibroproliferative response prevents ventricular rupture during the acute period following a transmural myocardial injury, we would propose that it is deleterious long term (10). Scar formation provides a barrier for regeneration as the milieu lacks the survival factors (i.e., vascularity, growth factors, and stem cells) necessary to promote and sustain cardiomyocyte repopulation (10, 33).

Our results should be compared with those reported by Leferovich et al. (21), who initially examined the regenerative capacity of the MRL adult mouse model. A number of technical differences exist between the two studies including the transdiaphragmatic cryoinjury involving the right ventricle, limited analysis of cardiac function, and an absence of molecular analysis in the previous study (21). In contrast, our study examined injuries involving the LV, an extensive functional analysis utilizing echocardiography in unanesthetized mice, and invasive hemodynamics complemented by a detailed molecular analysis. Nevertheless, both studies support the conclusion that the MRL mouse model has an improved reparative capacity and survival in response to myocardial injury.

In summary, the ability of the MRL mouse heart to regenerate is dependent upon the degree of injury that is produced. Furthermore, this animal model should prove useful for future studies directed toward cytoprotection and ventricular remodeling of the myopathic heart, as well as the application of therapeutic interventions that further promotes the regenerative process.

ACKNOWLEDGMENTS

The authors thank Dr. James Richardson, John Shelton, Dr. Cindy Martin, and Maggie Robledo for assistance with the histological, FACS, and surgical techniques. We acknowledge the assistance of Dr. Douglas F. Larson with the invasive hemodynamic measurements.

GRANTS

We acknowledge the funding support from the Donald W. Reynolds Foundation (D. J. Garry). D. J. Garry and M. G. Garry are Established Investigators of the American Heart Association.

REFERENCES

1. **Abdullah I, Lepore JJ, Epstein JA, Parmacek MS, Gruber PJ.** MRL mice fail to heal the heart in response to ischemia-reperfusion injury. *Wound Repair Regen* 13: 205–208, 2005.
2. **Balsam LB, Wagers AJ, Christensen JL, Kofidis T, Weissman IL, Robbins RC.** Haematopoietic stem cells adopt mature haematopoietic fates in ischaemic myocardium. *Nature* 428: 668–673, 2004.
3. **Beltrami AP, Barlucchi L, Torella D, Baker M, Limana F, Chimenti S, Kasahara H, Rota M, Musso E, Urbanek K, Leri A, Kajstura J, Nadal-Ginard B, Anversa P.** Adult cardiac stem cells are multipotent and support myocardial regeneration. *Cell* 114: 763–776, 2003.
4. **Beltrami AP, Urbanek K, Kajstura J, Yan SM, Finato N, Bussani R, Nadal-Ginard B, Silvestri F, Leri A, Beltrami CA, Anversa P.** Evidence that human cardiac myocytes divide after myocardial infarction. *N Engl J Med* 344: 1750–1757, 2001.
5. **Brockes JP, Kumar A.** Plasticity and reprogramming of differentiated cells in amphibian regeneration. *Nat Rev Mol Cell Biol* 3: 566–574, 2002.
6. **Brockes JP, Kumar A, Velloso CP.** Regeneration as an evolutionary variable. *J Anat* 199: 3–11, 2001.
7. **Clark LD, Clark RK, Heber-Katz E.** A new murine model for mammalian wound repair and regeneration. *Clin Immunol Immunopathol* 88: 35–45, 1998.
8. **Fuchs E, Segre JA.** Stem cells: a new lease on life. *Cell* 100: 143–155, 2000.
9. **Gallardo TD, Hammer RE, Garry DJ.** RNA amplification and transcriptional profiling for analysis of stem cell populations. *Genesis* 37: 57–63, 2003.
10. **Garry DJ, Martin CM.** Cardiac regeneration: self-service at the pump. *Circ Res* 95: 852–854, 2004.
11. **Garry DJ, Masino AM, Meeson AP, Martin CM.** Stem cell biology and therapeutic applications. *Curr Opin Nephrol Hypertens* 12: 447–454, 2003.
12. **Garry DJ, Meeson A, Elterman J, Zhao Y, Yang P, Bassel-Duby R, Williams RS.** Myogenic stem cell function is impaired in mice lacking the forkhead/winged helix protein MNF. *Proc Natl Acad Sci USA* 97: 5416–5421, 2000.
13. **Garwood J, Garcion E, Dobbertin A, Heck N, Calco V, ffrench-Constant C, Faissner A.** The extracellular matrix glycoprotein Tenascin-C is expressed by oligodendrocyte precursor cells and required for the regulation of maturation rate, survival and responsiveness to platelet-derived growth factor. *Eur J Neurosci* 20: 2524–2540, 2004.
14. **Glaser R, Lu MM, Narula N, Epstein JA.** Smooth muscle cells, but not myocytes, of host origin in transplanted human hearts. *Circulation* 106: 17–19, 2002.
15. **Goetsch SC, Hawke TJ, Gallardo TD, Richardson JA, Garry DJ.** Transcriptional profiling and regulation of the extracellular matrix during muscle regeneration. *Physiol Genomics* 14: 261–271, 2003.
16. **Harty M, Neff AW, King MW, Mescher AL.** Regeneration or scarring: an immunologic perspective. *Dev Dyn* 226: 268–279, 2003.
17. **Hawke TJ, Jiang N, Garry DJ.** Absence of p21CIP rescues myogenic progenitor cell proliferative and regenerative capacity in Foxk1 null mice. *J Biol Chem* 278: 4015–4020, 2003.
18. **Heber-Katz E.** The regenerating mouse ear. *Semin Cell Dev Biol* 4: 415–419, 1999.
19. **Jackson KA, Majka SM, Wang H, Pocius J, Hartley CJ, Majesky MW, Entman ML, Michael LH, Hirschi KK, Goodell MA.** Regeneration of ischemic cardiac muscle and vascular endothelium by adult stem cells. *J Clin Invest* 107: 1395–1402, 2001.
20. **Laflamme MA, Myerson D, Saffitz JE, Murry CE.** Evidence for cardiomyocyte repopulation by extracardiac progenitors in transplanted human hearts. *Circ Res* 90: 634–640, 2002.
21. **Leferovich JM, Bedelbaeva K, Samulewicz S, Zhang XM, Zwas D, Lankford EB, Heber-Katz E.** Heart regeneration in adult MRL mice. *Proc Natl Acad Sci USA* 98: 9830–9835, 2001.
22. **Martin CM, Meeson AP, Robertson SM, Hawke TJ, Richardson JA, Bates S, Goetsch SC, Gallardo TD, Garry DJ.** Persistent expression of the ATP-binding cassette transporter, Abcg2, identifies cardiac SP cells in the developing and adult heart. *Dev Biol* 265: 262–275, 2004.
23. **Masino AM, Gallardo TD, Wilcox CA, Olson EN, Williams RS, Garry DJ.** Transcriptional regulation of cardiac progenitor cell populations. *Circ Res* 95: 389–397, 2004.
24. **McBrearty BA, Clark LD, Zhang XM, Blankenhorn EP, Heber-Katz E.** Genetic analysis of a mammalian wound-healing trait. *Proc Natl Acad Sci USA* 95: 11792–11797, 1998.
25. **Meeson AP, Hawke TJ, Graham S, Jiang N, Elterman J, Hutcheson K, Dimaio JM, Gallardo TD, Garry DJ.** Cellular and molecular regulation of skeletal muscle side population cells. *Stem Cells* 22: 1305–1320, 2004.
26. **Murry CE, Soonpaa MH, Reinecke H, Nakajima H, Nakajima HO, Rubart M, Pasumarthi KB, Virag JI, Bartelmez SH, Poppa V, Bradford G, Dowell JD, Williams DA, Field LJ.** Haematopoietic stem cells do not transdifferentiate into cardiac myocytes in myocardial infarcts. *Nature* 428: 664–668, 2004.
27. **Nechiporuk A, Keating MT.** A proliferation gradient between proximal and msxb-expressing distal blastema directs zebrafish fin regeneration. *Development* 129: 2607–2617, 2002.
28. **Oh H, Bradfute SB, Gallardo TD, Nakamura T, Gaussin V, Mishina Y, Pocius J, Michael LH, Behringer RR, Garry DJ, Entman ML, Schneider MD.** Cardiac progenitor cells from adult myocardium: homing, differentiation, and fusion after infarction. *Proc Natl Acad Sci USA* 100: 12313–12318, 2003.
29. **Oh YS, Thomson LE, Fishbein MC, Berman DS, Sharifi B, Chen PS.** Scar formation after ischemic myocardial injury in MRL mice. *Cardiovasc Pathol* 13: 203–206, 2004.
30. **Orlic D, Kajstura J, Chimenti S, Jakoniuk I, Anderson SM, Li B, Pickel J, McKay R, Nadal-Ginard B, Bodine DM, Leri A, Anversa P.** Bone marrow cells regenerate infarcted myocardium. *Nature* 410: 701–705, 2001.
31. **Poss KD, Keating MT, Nechiporuk A.** Tales of regeneration in zebrafish. *Dev Dyn* 226: 202–210, 2003.
32. **Poss KD, Nechiporuk A, Hillam AM, Johnson SL, Keating MT.** Mps1 defines a proximal blastemal proliferative compartment essential for zebrafish fin regeneration. *Development* 129: 5141–5149, 2002.
33. **Poss KD, Wilson LG, Keating MT.** Heart regeneration in zebrafish. *Science* 298: 2188–2190, 2002.
34. **Ruiz C, Huang W, Hegi ME, Lange K, Hamou MF, Fluri E, Oakeley EJ, Chiquet-Ehrismann R, Orend G.** Growth promoting signaling by tenascin-C. *Cancer Res* 64: 7377–7385, 2004.
35. **Smith SA, Mammen PP, Mitchell JH, Garry MG.** Role of the exercise pressor reflex in rats with dilated cardiomyopathy. *Circulation* 108: 1126–1132, 2003.
36. **Taylor DA, Hruban R, Rodriguez ER, Goldschmidt-Clermont PJ.** Cardiac chimerism as a mechanism for self-repair: does it happen and if so to what degree? *Circulation* 106: 2–4, 2002.
37. **Van Empel VP, De Windt LJ.** Myocyte hypertrophy and apoptosis: a balancing act. *Cardiovasc Res* 63: 487–499, 2004.
38. **Weissman IL.** Stem cells: units of development, units of regeneration, and units in evolution. *Cell* 100: 157–168, 2000.
39. **Yang B, Larson DF, Watson R.** Age-related left ventricular function in the mouse: analysis based on in vivo pressure-volume relationships. *Am J Physiol Heart Circ Physiol* 277: H1906–H1913, 1999.